Angular dependence of Evanescent Field Enhancement on a glass-air interface

David Thompson

Abstract.

The purpose of this project was to determine experimentally the dependence on the angle of incidence of the enhancement of the evanescent field during total internal reflection. To achieve this a setup was realised to measure the emission by a fluorescent sample placed upon the planar surface of a semi-cylindrical lense, which was excited by a 467 nm diode laser over a wide range of incident angles. The fluorescent light was subsequently collected by an objective and the photon count was measured with the use of a lense focusing the light onto a Photomultiplier tube. As the near-field enhancement is dependent on the polarisation of the incident light, a linear polariser was placed between the source and te sample, and measurements were carried out for different polarisation states. The results of the s-polarisation measurements agree reasonably with the theory and are thus succesfull, the measurements under p-polarisation do not agree with theory, and will need further scrutiny.

Contents

Introduction.

This report discusses the findings of a project to measure the angular dependence of the near-field enhancement at sub and supercritical angles of incidence on a planar air-glass interface. The measurements were carried out specifically to confirm or disprove theoretical predictions of the aforementioned characteristics. The end result will be two curves, one for p-polarised incident light, and one for s-polarisation, of the light intensity due to fluorescence from the sample versus the angle of incidence.

The first part of the report focuses on theoretical aspects of the project, detailing the derivation of the equations giving rise to the theoretical curves, as well as some simulated figures to the same effect. Following this will be a discussion of the experimental methods used to achieve the goals set out in the preceding section. Here the different methods that came into consideration and were either pursued or abandoned will also be mentioned, with the reasoning behind their acceptance or rejection. The third section will then go into the actual measurements, and the processing of these measurements into the final results, including an analysis of the experimental errors that were encountered. The fourth and final section will then be used to draw some conclusions from the measurements, and to discuss possible improvements upon the experiment, to possibly facilitate further work in this area. A short overview of previous work related to this subject is also added at the end.

Theoretical aspects.

The phenomenon of total internal reflection (TIR) is well known and well understood. For an interface between a given material of refractive index n_1, and another material of lower index n_2, there exists a critical angle of incidence θ_{crit}. In general:

$$\theta_{crit} = \sin^{-1}\left(\frac{n_2}{n_1}\right) \qquad \textbf{(1)}$$

At and beyond this angle of incidence any incident light will be totally internally reflected, that is, no propagating light will be transmitted. However, as will be shown in a moment, there is still an electric field above the surface, which falls off exponentially along the z-axis, this is the evanescent field. The existence of the evanescent field can be found theoretically by the derivation of the Fresnel reflection and transmission coefficiënts, the final expressions for the coefficiënts are as follows[1]:

$$r^s(k_x, k_y) = \frac{\mu_2 k_{z1} - \mu_1 k_{z2}}{\mu_2 k_{z1} + \mu_1 k_{z2}} \qquad r^p(k_x, k_y) = \frac{\epsilon_2 k_{z1} - \epsilon_1 k_{z2}}{\epsilon_2 k_{z1} + \epsilon_1 k_{z2}} \qquad \textbf{(2)}$$

$$t^s(k_x, k_y) = \frac{2\mu_2 k_{z1}}{\mu_2 k_{z1} + \mu_1 k_{z2}} \qquad t^p(k_x, k_y) = \frac{2\epsilon_2 k_{z1}}{\epsilon_2 k_{z1} + \epsilon_1 k_{z2}} \sqrt{\frac{\mu_2 \epsilon_1}{\mu_1 \epsilon_2}} \qquad \textbf{(3)}$$

In these equations k_{z1} and k_{z2} are the components of the wavevectors in the two media along the z-axis. The x and y components of the wavevector are conserved accross the boundary, hence the z-components relate to them as follows:

$$k_{z1} = \sqrt{k_1^2 - (k_x^2 + k_y^2)} \qquad k_{z2} = \sqrt{k_2^2 - (k_x^2 + k_y^2)} \qquad \textbf{(4)}$$

Where k_1 and k_2 are of course the magnitudes of the wavevector before and after the interface respectively. For the purposes at hand it is most convenient to describe these in terms of the angle of incidence θ_i rather than the other wavevectors. This can be achieved by the fact that the transverse wavenumber can be expressed as:

$$k_{trans} = \sqrt{k_x^2 + k_y^2} = k_1 \sin\theta_i \qquad \textbf{(5)}$$

$$k_{z1} = k_1\sqrt{1 - \sin^2\theta_1} \quad \text{and} \quad k_{z2} = k_2\sqrt{1 - n_r^2 \sin^2\theta_1} \qquad \textbf{(6)}$$

where n_r is the relative index of refraction. The expression for θ_{crit} follows directly from the equation for k_{z2} should one equate the argument of the square root to zero. It is clear from this that, while it is indeed zero at the critical angle, after that k_{z2} becomes imaginary, leading to the evanescent wave. The relevant expression for the field directly above the glass surface can be acquired by simply applying these coëfficiënts to the incident E-field E_1, which leads to the following equations for the 3 spatial components of the evanescent field.

$$\vec{E}_2 = \begin{bmatrix} -iE_{1,p} t_p \sqrt{n_r^2 \sin^2\theta_1 - 1} \\ E_{1,s} t_s \\ E_{1,p} t_p n_r \sin\theta_1 \end{bmatrix} \cdot e^{-\gamma z} \qquad \textbf{(7)}$$

where $\gamma = k_2\sqrt{n_r^2 \sin^2\theta_1 - 1}$ is the decay constant.

This also shows that the polarisation state of the evanescent field depends on that of the the incident light. If the incident light is p - polarised, then the evanescent field is elliptically polarised in the x-z plane. In the case of s-polarised incident light the polarisation simply remains in that state.

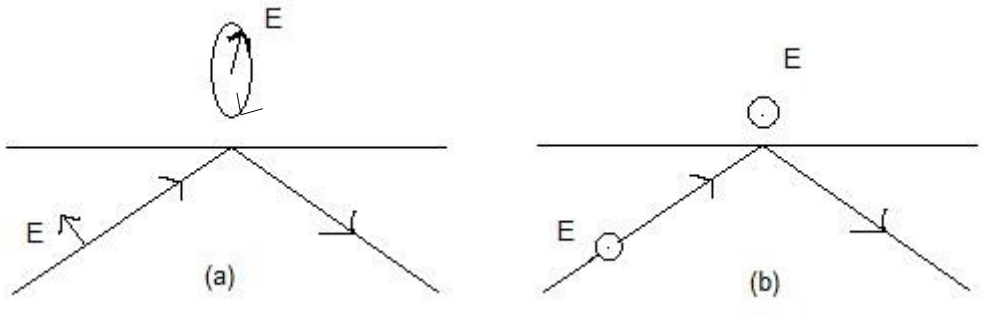

figure 1 - (a) shows the polarisation state of the evanescent field for p-polarised incident light, (b) for s-polarised incident light. [1],[2]

Equations 2-7 were subsequently used in the creation of a Matlab algorithm to plot the dependece of the evanescent field strength on both angle of incidence and distance z from the surface. The full algorithm can be found in appendix A, the following plots were obtained from this simulation.

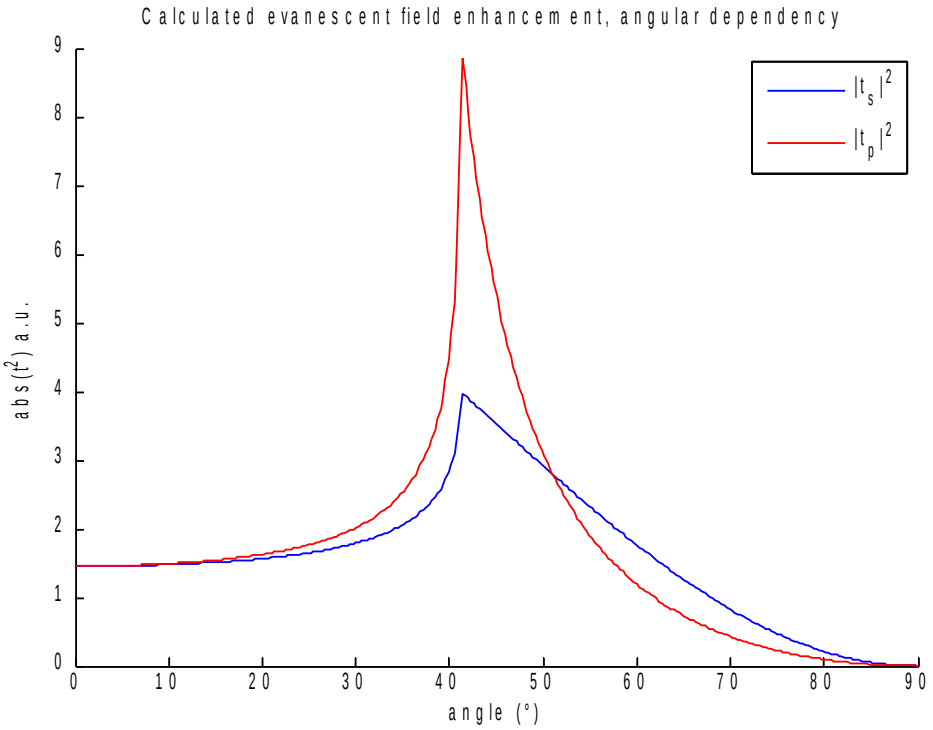

figure 2 - angular dependence of the near-field enhancement for s and p-polarisation states

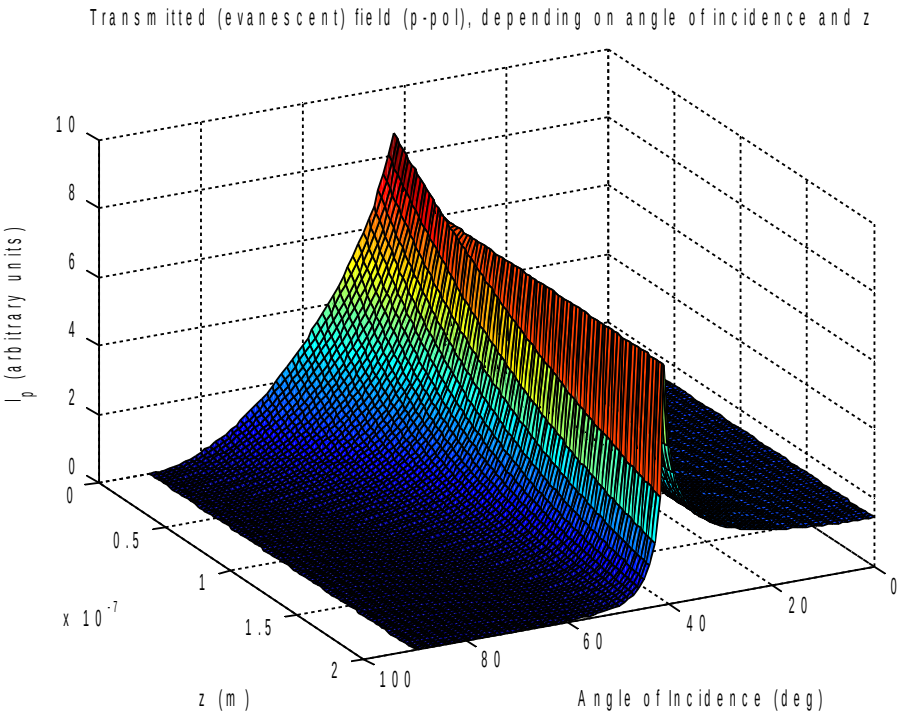

figure 3 - contour plot of the evanescent field dependence on angle of incidence and distance from the glass-air interface.

As can be seen in figure 2, the enhancement exhibits a peak at the critical angle for both polarisation states, but this peak is much more pronounced in the case of p-polarisation, and also falls off sharper in this case. In figure 3 the exponential decay of the field is nicely shown for supercritical angles, again, in keeping with what is expected.

Experimental aspects

In order to obtain an evanescent field that would remain stationary as θ_i is varied a setup involving a glass semi-cylinder was used. The incident light was delivered through a glass fibre which could be rotated on a stage around the cylinder. If the light enters the semi-cylinder normal to the curved surface it can be easily seen that it will exit through (and / or internally reflect off) the planar surface in the same location for all values of θ_i, which makes it easier to take reliable readings. A schematic of the entire setup is given in figure 4 below.

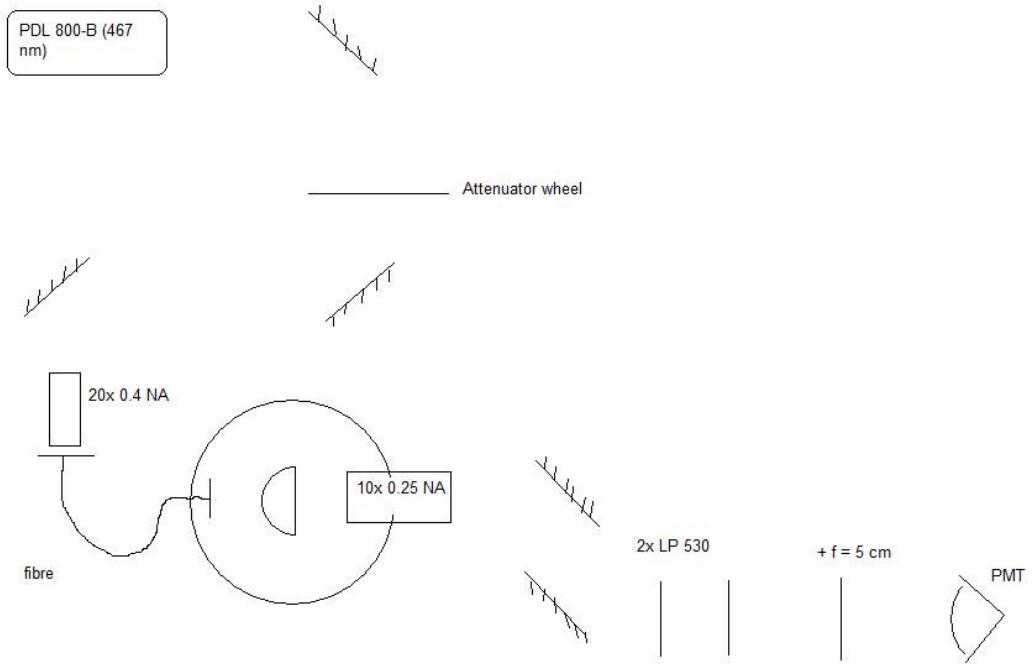

figure 4- schematic representation of the setup

The source used was a PicoQuant PDL 800-B diode laser, with an emmission wavelength of 467 nm. This source was first of all coupled into the optical fibre via three mirrors, the first of which was mainly used to redirect the reflection of the attenuator wheel, which was used to regulate the excitation strenght to at least some degree. The other two were to control the trajectory of the beam when coupling it into the 20x objective which was used to focus the light on the fibre's aperture. A photodiode and oscilloscope were used to optimise the coupling before moving on to the alignment of the rest of the setup. The fibre output can be rotated about the axis of the semi-cylinder, in order to achieve different incident angles. A polariser in front of the fibre output ensures the excitation light is linearly polarised, the polariser can be rotated to achieve s and p states. The fluorescence from the sample on the surface is collected by the 10x objective, from here two more mirrors, in a periscope-type configuration are used to guide the light to the detector. A pair of longpass coloured glass filters with a cut-on wavelenght of 530 nm are used to reduce noise from the excitation light, a positive lense with a focal length of 5 cm is used to focus the light onto the detection surface of the photomultiplier (Hamamatsu H 7421-40). The photomultiplier was connected to a Hameg HM 8021 counting module, which simply displays the counts/s.

Alignment.

In order to properly align the excitation light coming from the fibre (which incorporates a lense which keeps the beam narrow over a range of several centimeters) several steps had to be taken. First of all it was neccesary to find the axis of the cylinder. This was done with the use of a HeNe-

laser (alignment laser), incident from the detection side of the setup. This light partially reflects from the inside surface of the semi-cylinder, and thus it can be easily determined that the light from the alignment laser is normally incident on the flat surface, and indeed passes exaclty through the cylinder axis, when the reflected beam coincides with the incident beam at all times. This can be checked at the flat surface of the semi-cylinder, as well as both mirrors used to guide the light, and finally the alignment laser itself. Once this is done a reference point for aligning the excitation laser has been established. The next step was to get the excitation light to incide normally on the curved surface and pass through the axis at an incidence angle of 0º. This was done by adjusting the orientation and location of the fibre output until the excitation light followed a path parrallel to (or coinciding with, which one is not overly important) the alignment laser's. When this is the case you can be sure there is no refraction, so the excitation light is now properly incident for $\theta_1 = 0º$.

However this does not mean that the reflection spot on the flat surface is now in the same location for all values of θ_1. The angle of incidence on the curved surface can still vary, due to the distance between the edge of the rotation stage and the cylinder axis. This was first of all aligned to roughly the proper specifications purely by eyesight, using light scattered by the sample. After this a tabletop microscope (Nissho ZMS-50-1) was focused on the reflection spot in order to finetune the alignment. Making sure the spot created by the excitation light and the spot created by the alignment laser coincide at all angles finalises the alignment.

Measurement technique

Several methods for measuring this evanescent field were considered, the main two methods being NSOM (Near-field Scanning Optical Microscopy), and the application of a fluorescent sample to the surface of the semi-cylinder. Due to practical restrictions it was decided to proceed with the fluorescence measurements, for which a suitable sample was required.

Several types of fluorescent samples were considered, in the end, due to a lack of further time for measurements and failure of a previous sample, the measurements were carried out using a solution of 3.5 mg DCM in 1 mL of methanol. A droplet of 3 μL of this solution was deposited onto the planar surface fo the semi-cylinder, and left under a fume hood for approximately 15 minutes in order for the methanol to evaporate, leaving behind a deposit of reasonably evenly distributed DCM. The main aim was to have a sample that consisted of as little different components as possible, in order to minimise the possible variables that could affect the evanescent field itself. DCM has an absorption maximum at ~470 nm and an emission maximum at ~610 nm.[3]

As long as the sample is not saturated by the excitation light, the fluorescence responds to the exciting (evanescent) field in a linear manner. This means that the photon count measured by the PMT is directly proportional to the near-field enhancement, and thus need only be multiplied by a constant in order to check the agreement with the theoretical values.

Due to the sensitivity of the detector the setup needed to be shielded from any possible source of noise. Once ambient light is mostly blocked out, it must also be considered where the excitation light goes after TIR. It could well be that it reflects off one component or the other, meaning that it could end up disturbing the measurement, even if it might only happen (or beyond) at a certain angle of incidence.

Measurements

Measurements of the photon count from the sample fluorescence were taken for s-polarised and p-polarised incident light, the results are shown below, alongside the theoretical predictions for the values.

s-polarisation

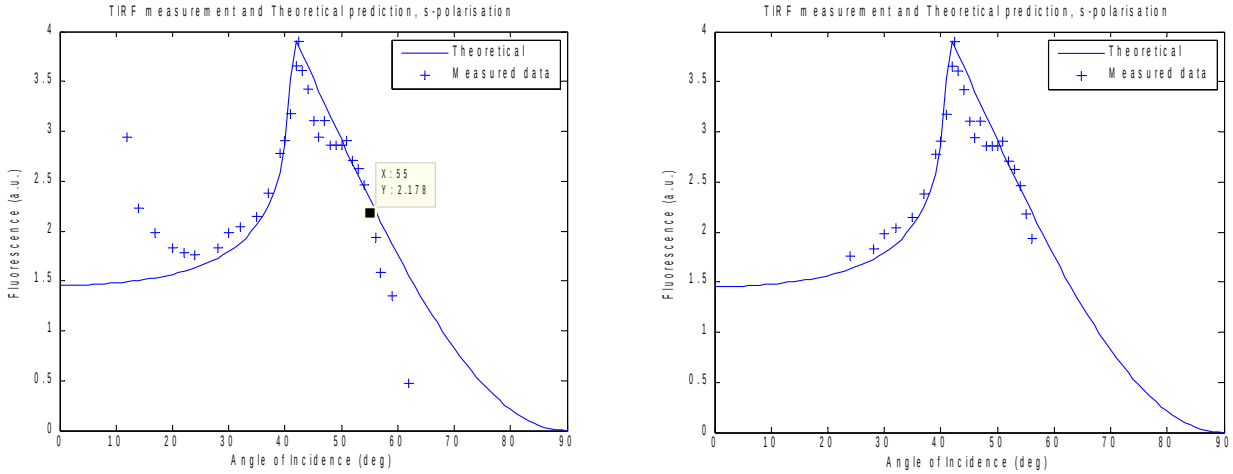

figure 5 - Measurements for s-polarisation, the figure on the left is composed of all the taken readings, the one on the right contains only the reliable datapoints.

As can be seen for the measurements for s-polarisation, the taken curve exhibits an increase in photon count from $\theta_1 < 20^\circ$, which does not correspond with the theory, as well as a steeper decrease than expected for $\theta_1 > 60^\circ$. This can be well explained by some of the characteristics of the setup itself, which caused these measurements to be deemed unreliable. At $\theta_1 < 20^\circ$ the excitation light does not yet refract sufficiently to bypass the collection objective, meaning a substantial amount of extra light is routed towards the detector.

The filters which were used are not sufficient to filter all of this light properly, at least partly due to the fact that they themselves fluoresce, leading to the increase in photon count for small angles of incidence. The steeper-than-expected decrease in photon count is due to an alignment problem, which causes the reflection spot to move somewhat to the right (from the detector's point of view), for sufficiently large angles, meaning the efficiency of the light collection would decrease, which manifests itself as a decrease in photon count larger than would be expected.

p-polarisation

Figure 7 shows the results for measurements with p-polarised incident light. As can be seen there is a major disagreement with the theory. Several possible causes for this were considered, such as the possible influence of absorption effects in the glass, or indeed within the sample itself. The sample was, after all, simply deposited directly in solution, meaning the residue after evaporation of the solvent probably consisted of more than a monolayer of DCM. These effects were studied by calculating what the evanescent field would look like if the refractive index of the glass were to be given an imaginary part, which would describe the absorption. If this is done both peaks will become smaller, and more spread out, not just one of them, meaning that, judging by the measurements made, it is unlikely that this was the cause of the problem.

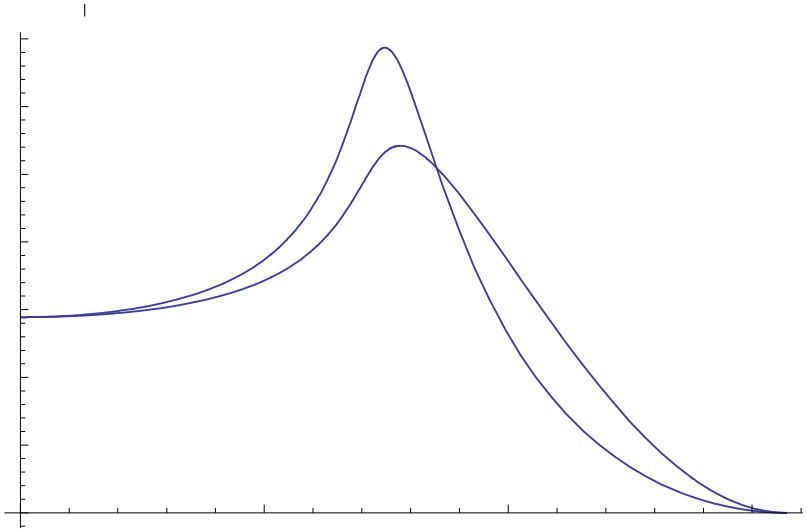

figure 6 - theoretical plot of the near-field enhancement voor both polarisations for refractive index $n_r = 1.5 + 0.1i$

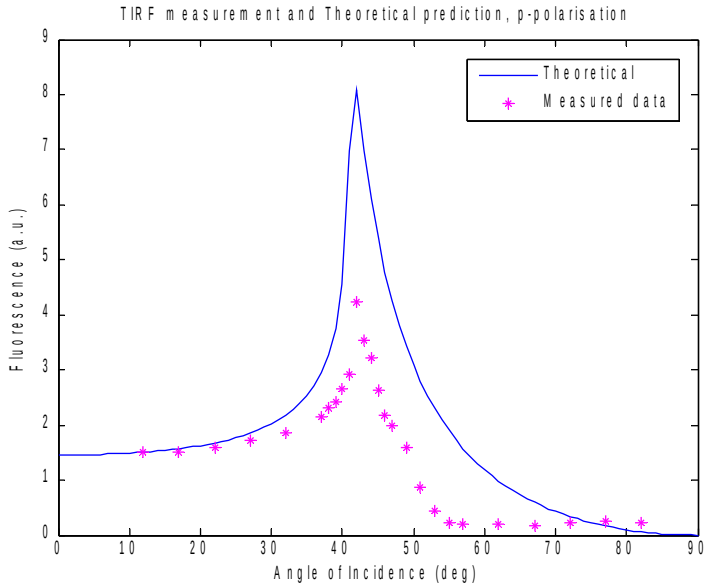

figure 7 - measurements for p-polarisation, as can be seen there is a major disagreement with the theory.

The most likely cause for the nature of the measurements has to do with the polarisation of the evanescent field, which is after all different depending on the polarisation of the incident light. In the case of s-polarised incident light the evanescent field remains in the same polarisation, this gives rise to emission dipoles oriented along that same axis.[4] The intensity distibution of the emission of these dipoles will be reasonably homogeneous in the x-z plane (no emmission along fluoresence axis, which on average is the y-axis), thus giving no problems in measuring with an objective oriented perpendicular to the surface. However in the case of p-polarised incident light, the evanescent field is elliptically polarised in the x-z plane, where the polarisation component in the z-direction is stronger than that in the x-direction. In this case the main components of the fluorescence axes of the molecules that are excited are in either the x-direction, or the z-direction (or somewhere inbetween). As the field amplitude is larger in the z-direction (see figure 1(a)), this would suggest that a majority of the fluorescence dipoles are excited along the z-axis. As the collection objective is also placed on the z-axis, this means that there will be a substantial loss of signal, as these dipoles aligned along the z-axis do not emit (a lot of) light in that direction (figure 8).

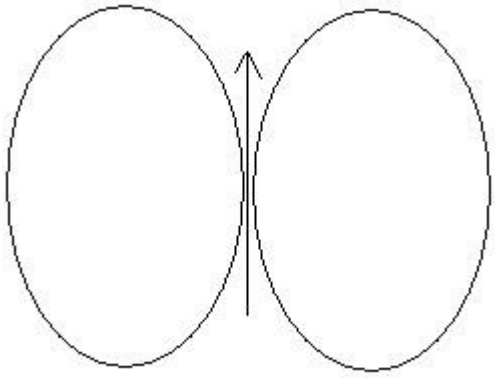

figure 8 - schematic representation of a fluorescence dipole, the arrow indicates the excitation axis, the ellipsses represent the direction of emission.

This could account for the fact that the peak in the measurements is a lot lower than would be expected, as the strength of the evanescent field increases, so does the amount of fluorophores excited along the z-axis, and proportionally less of the light will reach the detector.

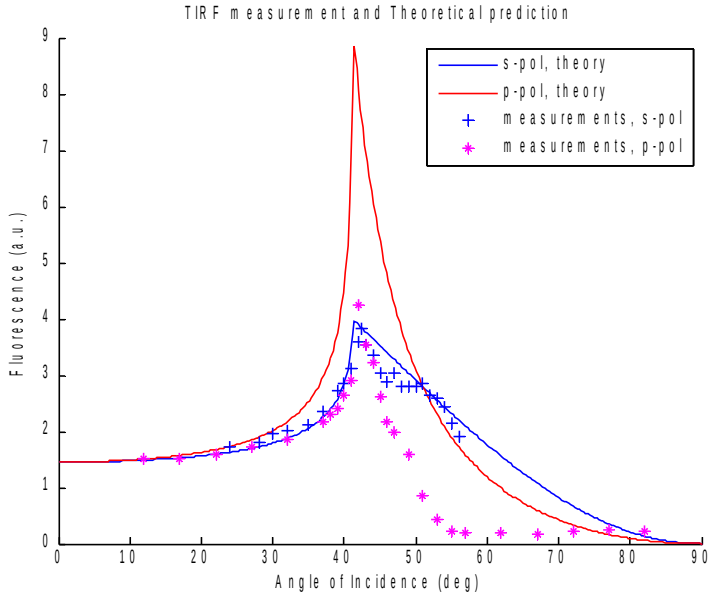

figure 9 - theory and measurements for both polarisations combined in one figure.

In figure 9 both results are compared to see to what extent the ratio of the evanscent field for the two different polarisations agrees with the theory. The value of the measured data for p-polarisation is clearly a lot lower than one would expect to find, showing more agreement with the curve for s-polarisation for subcritical angles of incidence, yet falling off more sharply at supercritical angles, which one would expect to see, but at higher values of the intensity.

Data processing and error analysis

In order to check the similarities and differences between the measured curves and the theoretical values all that needed to be done was to multiply the datapoints by a certain constant, that would fit them to one another. The way this was done was to take a datapoint in the lower range of θ_1 and dividing the corresponding theoretical value of the relevant $|r|^2$ by it, this number is the constant by which all the datapoints were multiplied. This is the only manipulation (apart from removing unreliable measurements in the case of s-polarisation) that was done on the data.

In the analysis of the measurement error only the error arising from fluctuations in the photon count were taken into account, as they were many times larger in magnitude than the errors intrinsic to the

counter and PMT. The errors in measurement were typically ± 3 kcounts/s, where the magnitude of the measurements themselves were typically in the order of 20 to 60 kcounts/s. Errors in the read-out of the angle (position of the rotation stage) were taken as ± 0.5º, an extra error of another 0.5º was added to the angle due to the necessity to establish a reference angle for $\theta_1 = 0º$. This turned out to be a position of the rotation stage of $\theta = 72.5º$ (± 0.5). After implementing these values for the possible errors the plot in figure 10 was found, leading to the conclusion that the measurements fall mostly within acceptable parameters, except for a few of the datapoints just beyond θ_{crit}. These discrepancies most likely arised due to some irregularity in the semi-cylinder, which may have led to some of the excitation light to be scattered to a larger degree than elsewhere in the glass.

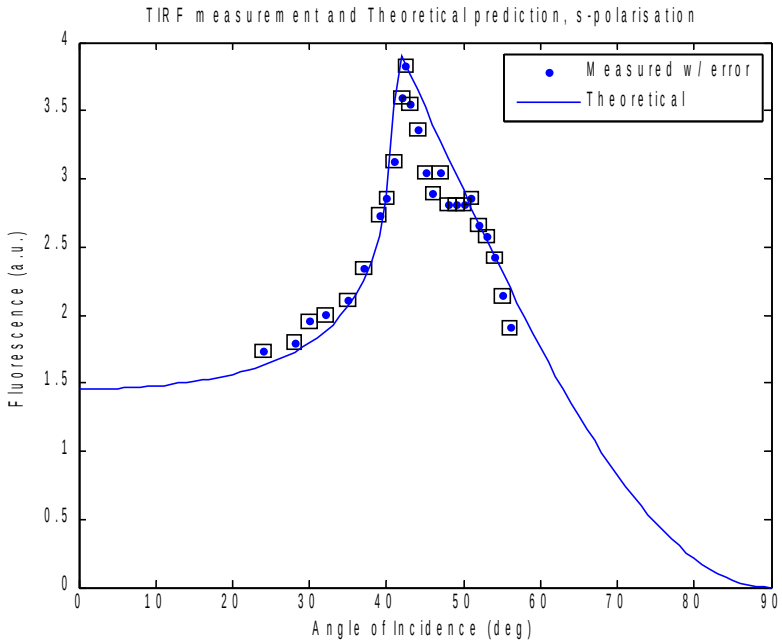

figure 10 - s-polarisation measurements with error boxes around the datapoints

The same analysis was of course applied to the measurements for p-polarisation, however here only the first 5 and last 3 datapoints were found to be in agreement with the theoretical curve, due to the intrinsic problems with these measurements.

Discussion

As was shown the measurements for s-polarised incident light agree substantially with the theory, whereas the measurements for p-polarisation do not. The most probable cause for this is the fact that fluorescence dipoles excited along a certain axis, do not emit light along that axis. This means that, for the elliptically polarised evanescent field which arises during the measurements for p-polarisation, a non-trivial part of the signal is lost due to the position of the detector along the z-axis. Several methods can be thought of to correct this error, and to further check the reliability of the measurements that were taken.

First of all one could measure, in the current setup, by exciting fluorescence at the same angles of incidence, but from the other side of the glass, meaning there is no evanescent field. In this case it would be expected that the fluorescence no longer shows a stron angular dependence, the curve of photon count vs. angle of incidence should be flat. If this is not the case, it could be inferred that some other effect than merely the evanescent field caused the observations that were made, which would render the experiment pointless, and some other method to measure the near-field should be used instead.

Knowing about the effects of the near-field polarisation on the fluorescence, a simple way to verify or disprove this would be to simply measure at another angle, somewhere inbetween the x and z axes. In this case there should no longer be a loss of signal, as in this case light from dipoles excited in either direction should reach the objective, now placed at an oblique angle, and through there the detector. A possible problem with this set-up would be that aligning the objective to collect as much light from the fluorescence as possible will be more difficult than in the current configuration, however it should be possible all the same. A definite advantage here would be that the objective could be placed so, that refracted excitation light at subcritical angles would never reach it, thus allowing for measurements at lower angles as well. In addition to these it would also seem to be a good idea to use a sample that is somewhat more precisely characterised than the one used in this experiment, so as to eliminate another uncertainty. Perhaps spincoating a monolayer of fluorescent nanospheres, embedded in some polymer would be advisable, provided the material the spheres are embedded in, or indeed the spheres themselves do not somehow perturb the field.

Finally a more direct way to measure the field may be in order, NSOM was already considered as a technique to use, and should work quite well. There are some considerations to this, however. Most importantly the semi-cylinder to be used would have to be of impeccable quality for the measurement to work over a large range of angles of incidence. Even a minor flaw in the curvature, of a minor deviation from being exactly half of a cylinder would cause the reflection spot to be moved at some point, causing a major signal loss at this point. It might be possible to devise a way around this problem by somehow moving the NSOM-tip along with the reflection spot, should it move, but this might be needlessly complicated.

Given the adaptations mentioned above, the fluorescence technique used to measure the near-field enhancement looks sound, and can be carried on.

Conclusions

For s-polarised incident light figures 5, 9 and 10 exhibit agreement with the theoretical curve, which leads to the reasonable assumption that the theory for p-polarisation should also be correct. The measurements for p-polarisation (figures 7 & 9) are, however, inconclusive at this time. At any rate both sets of measurements do confirm the fact that the near-field strength exhibits a definite maximum at the critical angle. This makes the theory all the more believable, and comprehensive measurements should follow soon after.

Papers related to the subject

A fair amount of previous work has been done in the area of TIRF, especially for biological purposes microscopy based in near-field fluorescence. A number of papers will be listed upon which some of this work was based, as well as some sources of information supporting the theory pertaining to the discrepancy in the p-polarisation measurement. For example an article from 1996 by Rahmani and De Fornel[5] demonstrates the near-field probing of fluorescent microspheres. Aside from using a setup very similar to the one used for this experiment, it is also a clear example of the sort of techniques used by biologists for near-field imaging. The exponential decay in the z-direction of the field is measured explicitly in an article from the Journal of Biomedical Optics from 2006 by Mattheyses and Axelrod[6], using objective-based TIRF measurements. A much earlier article from 1979 by Carniglia, Mandel and Drexhage[7] pertains to the absorption and emission of evanescent photons by a fluorescent sample. That article is of particular interest because the measurements deal with the absorption and emission probabilities of evanescent light, depending on the angle of incidence. They only carry out their measurements for s-polarised incident light, however the absorption figure in particular bears a striking resemblance to the figure for the near-field enhancement. The measurements for the emission of evanescent light by excited dye molecules also seem to be somewhat similar to the near-field enhancement, but to a much lesser degree.

Finally several articles[4],[8]-[13] were found that support the theory put forward pertaining to the disagreement between theory and this experiment for p-polarised incident light. The article by Burghardt and Thompson (in particular figure 2 is of use) treats the behaviour of fluorescent particles near a dielectric surface. In particular it shows that the traditional $\sin^2$ form of the directionality of the emission of a dipole is somewhat different near the surface, in that the emission is not completely zero at 0 and 180 degree angles of observation (relative to the dipole axis). The article by Cehelnik et.al provides a theoretical and mathematical description of the dependence of fluorescence emission on the polarisation of the exciting light relative to the dipole axis.

References

[1] L. Novotny & B. Hecht, *Priciples of Nano-optics*, Cambridge University Press 2006

[2] F. de Fornel, *Evanescent Waves From Newtonian Optics to Atomic Optics,* Springer-Verlag 2001

[3] S. Prahl, *PhotoCAD spectra, DCM in methanol,* Oregon Medical Laser Centre, http://omlc.ogi.edu/spectra/PhotochemCAD/html/dcm-pyran%28MeOH%29.html

[4] E.D. Cehelnik, K.D. Mielenz & R.A. Velapoldi, *Polarization effects on Fluorescence measurements,* Journal of Research of the National Bureau of Standards - A. Physics and Chemistry, Vol. 79A, Na. 1, January- February 1975

[5] A.Rahmani & F. de Fornel, *Near-field optical probing of fluorescent microspheres using a photon scanning tunneling microscope,* Optics Communications 131, 01-11-1996

[6] A.L. Mattheyses & D. Axelrod, *Direct measurement of the evanescent field profile produced by objective-based total internal reflection fluorescence,* Journal of Biomedical Optics 11, January/February 2006

[7] C.K. Carniglia, L. Mandel & K.H. Drexhage, *Absorption and emission of evanescent photons,* Journal of the Optical Society of America, volume 62, #4, April 1972

[8] T.P. Burghardt & N.L. Thompson, *Effect of Planar Dielectric Interfaces on Fluorescence Emission and Detection,* Biophys. J. V46 December 1984

[9] W.Lukosz, R.E. Kunz, *Light emission by magnetic and electric dipoles close to a plane interface*, Journal of the Optical Society of America, 1977

[10] W.Lukosz, R.E. Kunz, *Light emission by magnetic and electric dipoles close to a plane dielectric interface. II. Radiation patterns of perpendicular oriented dipoles,* Journal of the Optical Society of America, 1977

[11] D.Axelrod, E.H. Hellen & R.M. Fulbright, *Total Internal Reflection Fluorescence,* Topics in Fluorescence Spectroscopy, Volume 3: Biochemical Applications, 1992

[12] E.Lee, R. E. Benner, J. B. Fenn, & R. K. Chang, *Angular distribution of fluorescence from liquids and monodispersed spheres by evanescent wave excitation,* Applied Optics, Vol. 18, Issue 6, 1979

[13] A.L. Mattheyses & D. Axelrod, *Fluorescence emission patterns near glass and metal-coated surfaces investigated with back focal plane imaging*, Journal of Biomedical Optics, 2005

[14] S.M. Iftiquar, *Distribution of polarization vector for evanescent optical near-field*, Journal of Modern Optics, 55:11, 2008

[15] A.J. Meixner, M.A. Bopp & G. Tarrach, *Direct measurement of standing evanescent waves with a photon-scanning tunneling microscope,* Applied Optics, Vol. 33, No. 34, 1 December 1994

Appendix A

```
clear all
n_1 = 1.52;
n_2 = 1;
nrel = n_1/n_2;
Th_crit = asin(1/nrel);

E_1p = 1;
E_1s = 1;
E_1 = (E_1p+E_1s);

e_1 = nrel^2;
e_2 = 1;
mu_1 = 1;
mu_2 = 1;

labda = 467*10^-9;
k_1 = (2*pi/labda)*n_1;
k_2 = (2*pi/labda)*n_2;

zmax = 200*10^-9;
Th = 0:1:90;
z = 0:zmax/(length(Th)-1):zmax;
x = 0;

Th_1 = (Th.*pi)/180;
k_z_1 = k_1.*sqrt(1-sin(Th_1).^2);
k_z_2 = k_2.*sqrt(1-nrel^2*sin(Th_1).^2);
ts = zeros(1,length(Th));
tp = zeros(1,length(Th));

for n = 1:length(Th);
    ts(n) = ((2*mu_2*k_z_1(n))/(mu_2*k_z_1(n)+mu_1*k_z_2(n)));
    tp(n) = (((2*e_2*k_z_1(n))/(e_2*k_z_1(n)+e_1*k_z_2(n)))*sqrt((mu_2*e_1)/
(mu_1*e_2)));
end

y = k_2*sqrt(nrel^2*sin(Th_1).^2-1);


E_2p = zeros(size(Th));
E_2s = E_2p;

for a = 1:length(Th);
    E_2_Z(a) = E_1p.*tp(a).*nrel.*sin(Th_1(a));
    E_2_X(a) = -1i.*E_1p.*tp(a).*sqrt(nrel^2*sin(Th_1(a)).^2-1);
    E_2_Y(a) = E_1s.*ts(a);
    d(a) = (labda/(4*pi*n_2))*1/sqrt((sin(Th_1(a)).^2 - sin(Th_crit).^2));
    d2(a) = (labda/(4*pi*n_2))*1/sqrt((sin(Th_1(a))./sin(Th_crit)).^2-1);
    d3(a) = labda/(4*pi*sqrt(n_1.^2.*sin(Th_1(a)).^2-n_2.^2));
    for b = 1:length(z)
        E_2p_Z(b,a) = E_2_Z(a).*exp(1i*sin(Th_1(a))*k_1.*x).*exp(-y(a).*z(b));
        E_2p_X(b,a) = E_2_X(a).*exp(1i*sin(Th_1(a))*k_1.*x).*exp(-y(a).*z(b));
        E_2s(b,a) = E_2_Y(a).*exp(1i*sin(Th_1(a))*k_1.*x).*exp(-y(a).*z(b));
    end
end

I_p = abs(E_2p_Z).^2+abs(E_2p_X).^2; %Field intensity as result of purely p-
polarised incident light, eliptically polarised
I_s = abs(E_2s).^2; %Field intensity as a result of purely s-polarised incident
light, s-polarised
```

```
figure(1)
hold on
plot(Th, abs(ts).^2);
plot(Th, abs(tp).^2,'r');
xlabel('Angle of Incidence (deg)');
ylabel('|t|^2 (a.u.)')
title('Near-field enhancement dependent on angle of incidence')
hold off

figure(2)
surf(Th,z,I_s);
xlabel('Angle of Incidence (deg)');
ylabel('z (m)');
zlabel('I_p (arbitrary units)');
Title('Transmitted (evanescent) field (s-pol), depending on angle of incidence
and z');

figure(3)
surf(Th,z,I_p);
xlabel('Angle of Incidence (deg)');
ylabel('z (m)');
zlabel('I_p (arbitrary units)');
Title('Transmitted (evanescent) field (p-pol), depending on angle of incidence
and z');
```